

New Dry Friction Model with Load- and Velocity-Dependence and Dynamic Identification of Multi-DOF Robots

P. Hamon, M. Gautier, Philippe Garrec

► **To cite this version:**

P. Hamon, M. Gautier, Philippe Garrec. New Dry Friction Model with Load- and Velocity-Dependence and Dynamic Identification of Multi-DOF Robots. International Conference on Robotics and Automation, IEEE, May 2011, Shanghai, China. pp.1077-1084, 10.1109/ICRA.2011.5980126 . cea-01183057

HAL Id: cea-01183057

<https://hal-cea.archives-ouvertes.fr/cea-01183057>

Submitted on 6 Aug 2015

HAL is a multi-disciplinary open access archive for the deposit and dissemination of scientific research documents, whether they are published or not. The documents may come from teaching and research institutions in France or abroad, or from public or private research centers.

L'archive ouverte pluridisciplinaire **HAL**, est destinée au dépôt et à la diffusion de documents scientifiques de niveau recherche, publiés ou non, émanant des établissements d'enseignement et de recherche français ou étrangers, des laboratoires publics ou privés.

New Dry Friction Model with Load- and Velocity-Dependence and Dynamic Identification of Multi-DOF Robots

P. Hamon^(1,2), M. Gautier⁽²⁾, and P. Garrec⁽¹⁾

⁽¹⁾ CEA, LIST, Interactive Robotics Laboratory, 18 route du Panorama, BP6, Fontenay-aux-Roses, F-92265, France.

⁽²⁾ University of Nantes/IRCCyN, 1 rue de la Noë, BP 92101, Nantes Cedex 03, F-44321, France.

Abstract— Usually, the joint transmission friction model for robots is composed of a viscous friction force and of a constant dry sliding friction force. However, according to the Coulomb law, the dry friction force depends linearly on the load driven by the transmission, which has to be taken into account for robots working with large variation of the payload or inertial and gravity forces. Moreover, for robots actuating at low velocity, the Stribeck effect must be taken into account. This paper proposes a new inverse dynamic identification model for n degrees of freedom (dof) serial robot, where the dry sliding friction force is a linear function of both the dynamic and the external forces, with a velocity-dependent coefficient. A new sequential identification procedure is carried out. At a first step, the friction model parameters are identified for each joint (1 dof), moving one joint at a time (this step has been validated in [23]). At a second step, these values are fixed in the n dof dynamic model for the identification of all robot inertial and gravity parameters. For the two steps, the identification concatenates all the joint data collected while the robot is tracking planned trajectories with different payloads to get a global least squares estimation of inertial and new friction parameters. An experimental validation is carried out with an industrial 3 dof robot.

I. INTRODUCTION

THE usual identification method is based on the inverse dynamic model (IDM) which is linear in relation to the dynamic parameters, and uses least squares (LS) technique. This procedure has been successfully applied to identify inertial and friction parameters of a lot of prototypes and industrial robots [1]-[10]. An approximation of the sliding Coulomb friction, $F_C \text{sign}(\dot{q})$, is widely used to model friction force at non zero velocity \dot{q} , assuming that the friction force F_C is a constant parameter. It is identified by moving the robot without any load (or external force) or with constant given payloads [9].

However, the Coulomb law suggests that F_C depends on the transmission force driven in the mechanism. It depends on the dynamic and on the external forces applied through the joint drive chain. Consequently for robots with varying load, the identified IDM is no more accurate when the transmission uses industrial speed reducer, screw-nut or worm gear because their efficiency significantly varies with the transmitted force. The significant dependence on load has been often observed for transmission elements [15]-[19]

through direct measurement procedures. Moreover, the mechanism efficiency depends on the sense of power transfer leading to two distinct sets of friction parameters. In addition, when the robot moves at very low velocity, as for teleoperation, one observes a velocity-dependence of the dry friction.

This paper presents a new inverse dynamic identification model for n degrees of freedom (dof) serial robot, where the dry sliding friction force F_C is a linear function of both the dynamic and the external forces, with asymmetrical behavior depending on the signs of joint force and velocity, and a variation depending on the velocity amplitude. A new identification procedure is proposed. All the joint position and joint force data collected in several experiments, while the robot is tracking planned trajectories with different payloads, are concatenated to calculate a global least squares estimation of both the inertial and the new friction parameters.

An experimental validation is carried out on the 3 first joints of the Stäubli TX40 industrial robot [26].

II. USUAL INVERSE DYNAMIC MODELING AND IDENTIFICATION

A. Modeling

In the following, all mechanical variables are given in SI units in the joint space. All forces, positions, velocities and accelerations have a conventional positive sign in the same direction. That defines a motor convention for the mechanical behavior.

The dynamic model of a rigid robot composed of n moving links is written as follows [11]:

$$\tau_{dyn} = \tau + \tau_f + \tau_{off} + \tau_{ext} \quad (1)$$

where:

- τ_{dyn} is the $(n \times 1)$ vector of dynamic forces due to the inertial, centrifugal, Coriolis, and gravitational effects:

$$\tau_{dyn} = \mathbf{M}(q)\ddot{q} + \mathbf{C}(q, \dot{q})\dot{q} + \mathbf{Q}(q) \quad (2)$$

where q , \dot{q} and \ddot{q} are respectively the $(n \times 1)$ vectors of generalized joint positions, velocities and accelerations, $\mathbf{M}(q)$ is the $(n \times n)$ robot inertia matrix, $\mathbf{C}(q, \dot{q})$ is the $(n \times n)$ matrix of centrifugal and Coriolis effects, $\mathbf{Q}(q)$ is the $(n \times 1)$

vector of gravitational forces.

- $\boldsymbol{\tau}$ is the (nx1) input torque vector on the motor side of the drive chain, without offset:

$$\boldsymbol{\tau} = \mathbf{g}_f \mathbf{v}_f \quad (3)$$

where \mathbf{v}_f is the (nx1) vector of current references of the current amplifiers, \mathbf{g}_f is the (nxn) matrix of the drive gains.

- $\boldsymbol{\tau}_f$ is the (nx1) vector of the loss force due to viscous and dry frictions, without offset:

$$\boldsymbol{\tau}_f = -\mathbf{F}_V \dot{\mathbf{q}} - \mathbf{F}_C \text{sign}(\dot{\mathbf{q}}) \quad (4)$$

where \mathbf{F}_V is the (nxn) diagonal matrix of viscous parameters, \mathbf{F}_C is the (nxn) diagonal matrix of dry friction parameters, and $\text{sign}(\cdot)$ denotes the sign function (Fig. 1.a).

- $\boldsymbol{\tau}_{off}$ is an offset force that regroups the amplifier offset and the asymmetrical Coulomb friction coefficient.
- $\boldsymbol{\tau}_{ext}$ is the (nx1) external forces vector in the joint space.

Then (1) can be rewritten as the inverse dynamic model (IDM) which calculates the motor torque vector $\boldsymbol{\tau}$ as a function of the generalized coordinates:

$$\begin{aligned} \boldsymbol{\tau} &= \mathbf{M}(\mathbf{q})\ddot{\mathbf{q}} + \mathbf{C}(\mathbf{q}, \dot{\mathbf{q}})\dot{\mathbf{q}} + \mathbf{Q}(\mathbf{q}) + \mathbf{F}_C \text{sign}(\dot{\mathbf{q}}) + \mathbf{F}_V \dot{\mathbf{q}} + \boldsymbol{\tau}_{off} - \boldsymbol{\tau}_{ext} \quad (5) \\ &= \boldsymbol{\tau}_{out} + \mathbf{F}_C \text{sign}(\dot{\mathbf{q}}) + \mathbf{F}_V \dot{\mathbf{q}} + \boldsymbol{\tau}_{off} \end{aligned}$$

where $\boldsymbol{\tau}_{out} = \boldsymbol{\tau}_{dyn} - \boldsymbol{\tau}_{ext}$ is the output force (the load force) of the drive chain. For more details, see [23]

B. Identification

The choice of the modified Denavit and Hartenberg frames attached to each link allows to obtain a dynamic model linear in relation to a set of standard dynamic parameters $\boldsymbol{\chi}_{St}$ [6], [11]:

$$\boldsymbol{\tau} = \mathbf{D}_{St}(\mathbf{q}, \dot{\mathbf{q}}, \ddot{\mathbf{q}}) \boldsymbol{\chi}_{St} \quad (6)$$

where $\mathbf{D}_{St}(\mathbf{q}, \dot{\mathbf{q}}, \ddot{\mathbf{q}})$ is the regressor and $\boldsymbol{\chi}_{St}$ is the vector of the standard parameters which are the coefficients $XX_j, XY_j, XZ_j, YY_j, YZ_j, ZZ_j$ of the inertia tensor of link j denoted ${}^j\mathbf{J}_j$, the mass of the link j called m_j , the first moments vector of link j around the origin of frame j denoted ${}^j\mathbf{M}_j = [MX_j \ MY_j \ MZ_j]^T$, the friction coefficients F_{Vj}, F_{Cj} , the actuator inertia called Ia_j , and the offset τ_{offj} . The velocities and accelerations are calculated using well tuned band pass filtering of the joint position [7].

The base parameters are the minimum number of parameters from which the dynamic model can be calculated. They are obtained by eliminating and by regrouping some standard inertial parameters [12], [13]. The minimal inverse dynamic model can be written as:

$$\boldsymbol{\tau} = \mathbf{D}(\mathbf{q}, \dot{\mathbf{q}}, \ddot{\mathbf{q}}) \boldsymbol{\chi} \quad (7)$$

where $\mathbf{D}(\mathbf{q}, \dot{\mathbf{q}}, \ddot{\mathbf{q}})$ is the minimal regressor and $\boldsymbol{\chi}$ is the vector

of the base parameters.

The inverse dynamic model (7) is sampled while the robot is tracking a trajectory to get an over-determined linear system such that [6]:

$$\mathbf{Y}(\boldsymbol{\tau}) = \mathbf{W}(\mathbf{q}, \dot{\mathbf{q}}, \ddot{\mathbf{q}}) \boldsymbol{\chi} + \boldsymbol{\rho} \quad (8)$$

with $\mathbf{Y}(\boldsymbol{\tau})$ the measurements vector, \mathbf{W} the observation matrix and $\boldsymbol{\rho}$ the vector of errors.

The LS solution $\hat{\boldsymbol{\chi}}$ minimizes the 2-norm of the vector of errors $\boldsymbol{\rho}$. \mathbf{W} is a (rxb) full rank and well conditioned matrix where $r = N_e \times n$, with N_e the number of samples on the trajectories. The LS solution $\hat{\boldsymbol{\chi}}$ is given by:

$$\hat{\boldsymbol{\chi}} = (\mathbf{W}^T \mathbf{W})^{-1} \mathbf{W}^T \mathbf{Y} = \mathbf{W}^+ \mathbf{Y} \quad (9)$$

It is calculated using the QR factorization of \mathbf{W} . Standard deviations $\sigma_{\hat{\chi}_i}$ are estimated using classical and simple results from statistics. The matrix \mathbf{W} is supposed to be deterministic, and $\boldsymbol{\rho}$, a zero-mean additive independent noise, with a standard deviation such as:

$$\mathbf{C}_{\rho\rho} = \mathbf{E}(\boldsymbol{\rho}\boldsymbol{\rho}^T) = \sigma_\rho^2 \mathbf{I}_r \quad (10)$$

where \mathbf{E} is the expectation operator and \mathbf{I}_r , the (rxr) identity matrix. An unbiased estimation of σ_ρ is:

$$\hat{\sigma}_\rho^2 = \|\mathbf{Y} - \mathbf{W}\hat{\boldsymbol{\chi}}\|^2 / (r - b) \quad (11)$$

The covariance matrix of the standard deviation is calculated as follows:

$$\mathbf{C}_{\hat{\chi}\hat{\chi}} = \mathbf{E}[(\boldsymbol{\chi} - \hat{\boldsymbol{\chi}})(\boldsymbol{\chi} - \hat{\boldsymbol{\chi}})^T] = \sigma_\rho^2 (\mathbf{W}^T \mathbf{W})^{-1} \quad (12)$$

$\sigma_{\hat{\chi}_i}^2 = C_{\hat{\chi}\hat{\chi}ii}$ is the i^{th} diagonal coefficient of $\mathbf{C}_{\hat{\chi}\hat{\chi}}$. The relative standard deviation $\% \sigma_{\hat{\chi}_i}$ is given by:

$$\% \sigma_{\hat{\chi}_i} = 100 \sigma_{\hat{\chi}_i} / \hat{\chi}_i \quad (13)$$

However, experimental data are corrupted by noise and error modeling and \mathbf{W} is not deterministic. This problem can be solved by filtering the measurement vector \mathbf{Y} and the columns of the observation matrix \mathbf{W} as described in [7], [8].

III. NEW DRY FRICTION MODEL AND IDENTIFICATION

In this section, we introduce a dry friction model dependent on the load, that is $\boldsymbol{\tau}_{out}$, and on the velocity $\dot{\mathbf{q}}$. This model is more detailed in [23] (see also [24]).

A. Load- and Velocity-Dependent Friction Model

The Coulomb friction is still written $\mathbf{F}_C \text{sign}(\dot{\mathbf{q}})$, with \mathbf{F}_C a (nxn) diagonal matrix.

But here, for each link j , F_{Cj} (the $(j,j)^{\text{th}}$ element of the matrix \mathbf{F}_C) depends linearly on the absolute value of the

load of joint j which is $\tau_{out j}$ (Fig. 1.b), [15]-[19]:

$$F_{Cj} = \alpha_j |\tau_{out j}| + \beta_j \quad (14)$$

At low velocity, taking into account the Stribeck effect improves the model accuracy, [20]-[22]:

$$F_{Cj} = F_{slj} + (F_{stj} - F_{slj})e^{-|\dot{q}_j/\dot{q}_s|} \quad (15)$$

where \dot{q}_{sj} is a velocity constant, F_{stj} is the dry friction in stiction and F_{slj} is the dry friction in sliding mode.

To combine both load (14) and velocity (15) variations one takes:

$$F_{slj} = \alpha_j |\tau_{out j}| + \beta_j \quad \text{and} \quad F_{stj} = \gamma_j |\tau_{out j}| + \delta_j \quad (16)$$

Then, the dry friction model becomes (Fig. 1.c):

$$F_{Cj} = \alpha_j |\tau_{out j}| + \beta_j + (\gamma_j |\tau_{out j}| + \delta_j - \alpha_j |\tau_{out j}| - \beta_j)e^{-|\dot{q}_j/\dot{q}_s|} \quad (17)$$

where α_j , β_j , γ_j and δ_j are parameters to be identified. These new parameters depend on the mechanical structure of the reducers used to actuate the robot.

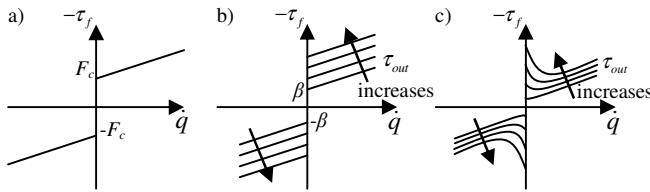


Fig. 1. a) Usual friction model with constant dry friction + viscous friction. b) Model with load-dependent dry friction + viscous friction. c) Model with load- and velocity-dependent dry friction + viscous friction.

To simplify, by using $|\tau_{out j}| = \tau_{out j} \text{sign}(\tau_{out j})$ and $\text{sign}(\tau_{out j}) \text{sign}(\dot{q}_j) = \text{sign}(\tau_{out j} \dot{q}_j) = \text{sign}(P_{out j})$, one obtains:

$$F_{Cj} \text{sign}(\dot{q}_j) = \left(\alpha_j + (\gamma_j - \alpha_j)e^{-|\dot{q}_j/\dot{q}_s|} \right) \tau_{out j} \text{sign}(P_{out j}) + \dots \dots \left(\beta_j + (\delta_j - \beta_j)e^{-|\dot{q}_j/\dot{q}_s|} \right) \text{sign}(\dot{q}_j) \quad (18)$$

For each joint, the frame $(\dot{q}_j, \tau_{out j})$ is divided in 4 quadrants which can be grouped two by two (Fig. 2.a). In the quadrants 1 and 3, the output power $P_{out j}$ is positive and the actuator has a motor behavior. In the quadrants 2 and 4, $P_{out j}$ is negative and the actuator has a generator behavior.

In the model (18), α_j , β_j , γ_j and δ_j take generally different values depending on the actuator behavior: α_{mj} , β_{mj} , γ_{mj} and δ_{mj} for the motor quadrants, and α_{gj} , β_{gj} , γ_{gj} and δ_{gj} for the generator quadrants. See Fig. 2.b: illustration of (19) with (14) for a constant velocity $|\dot{q}_0|$, and 2 different sets of friction parameters (motor and generator), in frame (τ, τ_{out}) .

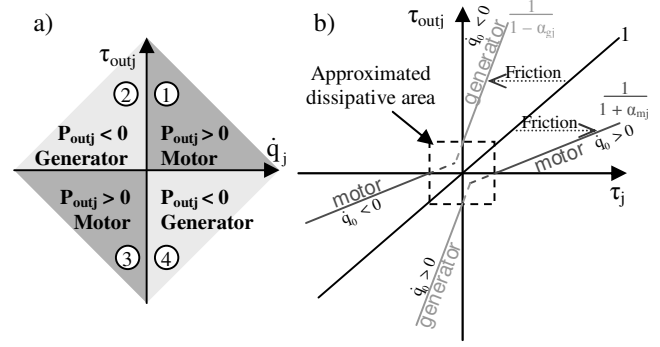


Fig. 2. a) Four quadrants frame $(\dot{q}_j, \tau_{out j})$ for motor or generator behavior. b) Asymmetrical friction for a given velocity \dot{q}_0 and the stiction area.

For each joint j , the dynamic model can be written as follows:

$$\tau_j = \tau_{out j} + F_{Cj} \text{sign}(\dot{q}_j) + F_{Vj} \dot{q}_j + \tau_{off j} \quad (19)$$

Considering

$$a_{mj} = \gamma_{mj} - \alpha_{mj}, b_{mj} = \delta_{mj} - \beta_{mj}, a_{gj} = \gamma_{gj} - \alpha_{gj}, \quad \text{and} \quad b_{gj} = \delta_{gj} - \beta_{gj},$$

the inverse dynamic model for joint j is written with 2 expressions and becomes:

$$\begin{cases} \bullet P_{out j} > 0 \Rightarrow \tau_j = (1 + \alpha_{mj}) \tau_{out j} + a_{mj} \tau_{out j} e^{-|\dot{q}_j/\dot{q}_s|} + \dots \\ \dots + \beta_{mj} \text{sign}(\dot{q}_j) + b_{mj} e^{-|\dot{q}_j/\dot{q}_s|} \text{sign}(\dot{q}_j) + F_{Vj} \dot{q}_j + \tau_{off j} \\ \bullet P_{out j} < 0 \Rightarrow \tau_j = (1 - \alpha_{gj}) \tau_{out j} - a_{gj} \tau_{out j} e^{-|\dot{q}_j/\dot{q}_s|} + \dots \\ \dots + \beta_{gj} \text{sign}(\dot{q}_j) + b_{gj} e^{-|\dot{q}_j/\dot{q}_s|} \text{sign}(\dot{q}_j) + F_{Vj} \dot{q}_j + \tau_{off j} \end{cases} \quad (20)$$

B. Friction Identification Method

In order to keep a model linear in relation to the parameters and to use the linear least square method, one has an identification in 3 steps.

At a **first** step, \dot{q}_{sj} is identified with the measurements of several constant velocities trajectories: the amplitude of the transitional behavior, on the graph of the mean input torque with respect to the mean velocity (Fig. 4), is 3 times \dot{q}_{sj} . One introduces a new variable $E_{xp j}$, defined by:

$$E_{xp j} = e^{-|\dot{q}_j/\dot{q}_s|} \quad (21)$$

At a **second** step, one identifies each joint separately to obtain especially the values of the friction parameters of each joint. However, the model (20) depends on the sign of $P_{out j}$ which is unknown. To overcome this problem, the samples of τ measurements are selected outside of the dissipative area (Fig. 2.b) in order to get the same sign for $\tau_{out j}$ and τ_j . This allows to get the sign of $P_{out j}$ with:

$$\text{sign}(P_{out j}) = \text{sign}(\tau_{out j} \dot{q}_j) = \text{sign}(\tau_j \dot{q}_j) = \text{sign}(P_j) \quad (22)$$

One can then write the IDM linear in relation to parameters and use the LS technique. To have only one

expression instead of two in (20), 2 variables are introduced, P_j^+ and P_j^- defined by:

$$P_j^+ = \frac{1 + \text{sign}(P_j)}{2}, P_j > 0 \Leftrightarrow P_j^+ = 1, P_j < 0 \Leftrightarrow P_j^+ = 0 \quad (23)$$

$$P_j^- = \frac{1 - \text{sign}(P_j)}{2} = \bar{P}_j^+ \quad (24)$$

The inverse dynamic model of joint j is then written:

$$\begin{aligned} \tau_j = & P_j^+ (I + \alpha_{mj} + a_{mj} E_{xpj}) \tau_{outj} + P_j^- (I - \alpha_{gj} - a_{gj} E_{xpj}) \tau_{outj} + \dots \\ & \dots P_j^+ (\beta_{mj} + b_{mj} E_{xpj}) \text{sign}(\dot{q}_j) + P_j^- (\beta_{gj} + b_{gj} E_{xpj}) \text{sign}(\dot{q}_j) + \dots \quad (25) \\ & \dots F_{Vj} \dot{q}_j + \tau_{offj} \end{aligned}$$

τ_{outj} is linear in relation to inertial and gravity parameters and can be written $\tau_{outj} = D_{outj} \chi_{outj}$. For a known value \dot{q}_{Sj} (from step 1), the variable (21) allows to obtain a linear identification model (25) where the parameters to identify are: $(I + \alpha_{mj}) \chi_{outj}$, $a_{mj} \chi_{outj}$, $(I - \alpha_{gj}) \chi_{outj}$, $a_{gj} \chi_{outj}$, and all the friction parameters alone. By using exciting trajectories and the LS technique, one can then obtain the values of α_{mj} , a_{mj} , α_{gj} , and a_{gj} .

The same method, with products of parameters to have a linear model, is hard to apply to a multi-dof robot as the number of parameters to identify would increase a lot with the number of joints (for example, with the 3 dof robot here: 15 parameters for the usual model will give 67 parameters for the new one). That is why the second step is needed to identify the friction parameters alone, and set their values for the third step: the multi-dof identification.

At a **third** step, the values of \dot{q}_{Sj} , α_{mj} , a_{mj} , α_{gj} , and a_{gj} of each joint are added in the global observation matrix of the robot W . Then, the global inverse dynamic model is linear in relation to the inertial and gravity parameters, and to the parameters β_m , b_m , β_g , b_g , F_V (which are all (nxn) diagonal matrices) and τ_{off} . All these parameters can be identified.

IV. EXPERIMENTAL SETUP AND IDENTIFICATION

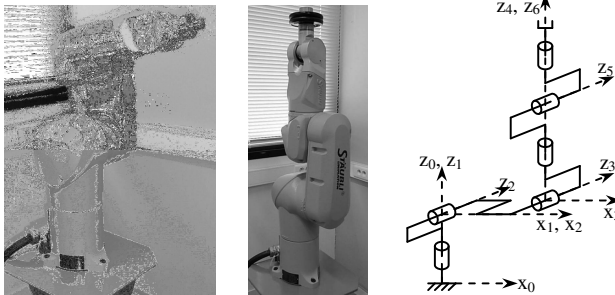


Fig. 3. The Stäubli TX40 Robot: picture without payload, picture with 1.195 kg payload, and drawing with frame for each joint.

A. Study case: Stäubli TX40 Robot

The Stäubli TX40 robot (Fig. 3) is an industrial robot with 6 rotational joints. The 3 first joints are studied here and the links 4, 5 and 6 are locked in position 0.

The nominal velocity is 5.01 rad/s for the joints 1 and 2, and 7.52 rad/s for the joint 3. The maximum acceptable load at the extremity is about 2 kg.

B. Data Acquisition

The identification of dynamic parameters is carried out with and without payloads: five different additional masses can be fixed to the arm extremity. To excite properly the friction parameters to be identified, sinusoidal and trapezoidal velocities trajectories were used.

The estimation of \dot{q} and \ddot{q} are carried out with pass band filtering of q consisting of a low pass Butterworth filter and a central derivative algorithm. The Matlab function *filtfilt* can be used [25]. The motor torque is calculated using the current reference (3). In order to cancel high frequency ripple in τ , the vector Y and the columns of the observation matrix W are both low pass filtered and decimated. This parallel filtering procedure is carried out with the Matlab *decimate* function [2], [10].

C. First Identification Step

As the Stribeck effect is increased when the joint is loaded, one takes for each joint the measurements with the highest load (positive and negative) and for several constant velocities (positive and negative) to observe the amplitude of the exponential transient behavior. For each joint, \dot{q}_{Sj} is measured on the graph of the input torque functions of the velocity (Fig. 4): $\dot{q}_{S1} = 0.1$, $\dot{q}_{S2} = 0.1$, and $\dot{q}_{S3} = 0.15$.

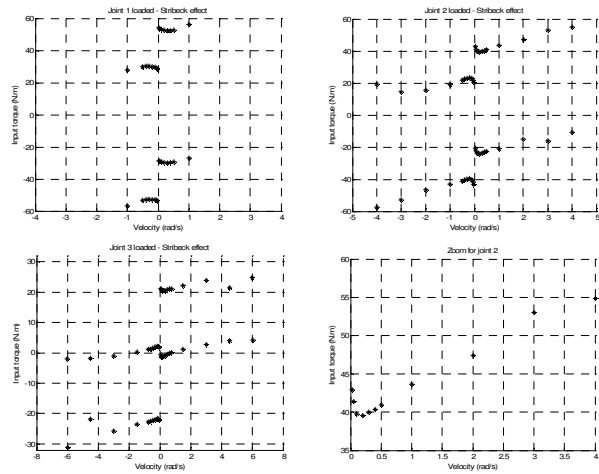


Fig. 4. Graphs of the Stribeck effect: joints 1, 2, and 3, and zoom for joint 2

D. Second Identification Step

Each joint j is identified alone to obtain the values of α_{mj} , a_{mj} , α_{gj} , and a_{gj} . To identify the load-dependent friction, measurements with known payloads are used and the robot

configuration is chosen so that the load variation is bigger. Gravity and inertial forces due to the additional mass fixed to the robot extremity have to be added in the IDM. Details are given for the joint 2: the measurements are done with the link 3 aligned with link 2 (all links are locked except for the 2nd). And the inverse dynamic model of joint 2 is given by:

$$\begin{aligned} \tau_2 = & J_2 \ddot{q}_2 + MX_{R2} g \cos(q_2) + MY_{R2} g \sin(q_2) + M_{a(k)} L_{a(k)}^2 \ddot{q}_2 + \dots \\ & \dots M_{a(k)} L_{a(k)} g \cos(q_2) + F_{C2} \text{sign}(\dot{q}_2) + F_{V2} \dot{q}_2 + \tau_{\text{off}2} \end{aligned} \quad (26)$$

where:

- $J_2 = Ia_2 + ZZ_{R2}$ is the inertia moment Ia_2 of the drive chain plus the inertia moment ZZ_{R2} of the arm,
- ZZ_{R2} , MX_{R2} , MY_{R2} are the inertial parameters of link 2 regrouped with those of link 3 to 6 which are locked,
- $g = 9.81 \text{ m/s}^2$ is the gravity acceleration,
- $M_{a(k)}$ ($k \in [1:5]$) is the mass of one of the five additional payloads, with accurate weighed values: 0.00 kg, 0.6744 kg, 1.1955 kg, 1.6990 kg, and 2.2173 kg,
- $L_{a(k)}$ is the length from the joint 2 to the gravity center of the mass of the additional payload (measured distances): 0.00 m, 0.5335 m, 0.5395 m, 0.5465 m, and 0.5415 m.

All variables and parameters are given in SI units on the joint space.

One defines $\tau_{ma2(k)}$ which is the output torque due to the additional payload k , applied on joint 2:

$$\tau_{ma2(k)} = M_{a(k)} L_{a(k)} (L_{a(k)} \ddot{q}_2 + g \cos(q_2)) \quad (27)$$

Then, $\tau_{\text{out}2}$ is defined by:

$$\tau_{\text{out}2} = J_2 \ddot{q}_2 + MX_2 g \cos(q_2) + MY_2 g \sin(q_2) + \tau_{ma2} \quad (28)$$

and the IDM of joint 2 with the proposed friction model is written as in (25):

$$\begin{aligned} \tau_2 = & (P_2^+ (1 + \alpha_{m2} + a_{m2} E_{xp2}) + P_2^- (1 - \alpha_{g2} - a_{g2} E_{xp2})) \tau_{\text{out}2} + \dots \\ & \dots P_2^+ (\beta_{m2} + b_{m2} E_{xp2}) \text{sign}(\dot{q}_2) + P_2^- (\beta_{g2} + b_{g2} E_{xp2}) \text{sign}(\dot{q}_j) + \dots \quad (29) \\ & \dots F_{V2} \dot{q}_2 + \tau_{\text{off}2} \end{aligned}$$

One takes a linear form of this IDM and it is identified (a comparison of the results can be made with the usual friction model but is not detailed here. See [23]). The sampled measurements, for k from 1 to 5, are concatenated using the $\tau_{ma2(k)}$ corresponding to all experiments k with the motor torques $\tau_{2(k)}$, to get the linear system:

$$Y_2 = W_2 \chi_2 + \rho_2 \quad (30)$$

with the measurements vector, the observation matrix, and the vector of base parameters defined as follows:

$$Y_2 = \tau_2 = \begin{bmatrix} \tau_{2(1)}^T & \tau_{2(2)}^T & \tau_{2(3)}^T & \tau_{2(4)}^T & \tau_{2(5)}^T \end{bmatrix}^T \quad (31)$$

$$\begin{aligned} W_2 = & \begin{bmatrix} P_2^+ \ddot{q}_2 & P_2^+ E_{xp2} \ddot{q}_2 & P_2^+ g \cos(q_2) & \dots \\ \dots & P_2^+ E_{xp2} g \cos(q_2) & P_2^+ g \sin(q_2) & P_2^+ E_{xp2} g \sin(q_2) & \dots \\ \dots & P_2^+ \tau_{ma2} & P_2^+ E_{xp} \tau_{ma2} & P_2^- \ddot{q}_2 & -P_2^- E_{xp2} \ddot{q}_2 & P_2^- g \cos(q_2) & \dots \\ \dots & -P_2^- E_{xp2} g \cos(q_2) & P_2^- g \sin(q_2) & -P_2^- E_{xp2} g \sin(q_2) & \dots \\ \dots & P_2^- \tau_{ma2} & -P_2^- E_{xp2} \tau_{ma2} & P_2^+ \text{sign}(\dot{q}_2) & P_2^+ E_{xp2} \text{sign}(\dot{q}_2) & \dots \\ \dots & P_2^- \text{sign}(\dot{q}_2) & P_2^- E_{xp2} \text{sign}(\dot{q}_2) & \dot{q}_2 & I \end{bmatrix} \end{aligned} \quad (32)$$

$$\begin{aligned} \chi_2 = & \begin{bmatrix} (1 + \alpha_{m2}) J_2 & a_{m2} J_2 & (1 + \alpha_{m2}) MX_{R2} & a_{m2} MX_{R2} & (1 + \alpha_{m2}) MY_{R2} & \dots \\ \dots & a_{m2} MY_{R2} & 1 + \alpha_{m2} & a_{m2} & (1 - \alpha_{g2}) J_2 & a_{g2} J_2 & (1 - \alpha_{g2}) MX_{R2} & \dots \\ \dots & a_{g2} MX_{R2} & (1 - \alpha_{g2}) MY_{R2} & a_{g2} MY_{R2} & 1 - \alpha_{g2} & a_{g2} & \dots \\ \dots & \beta_{m2} & b_{m2} & \beta_{g2} & b_{g2} & F_{V2} & \tau_{\text{off}2} \end{bmatrix}^T \end{aligned} \quad (33)$$

Here P_2^+ , P_2^- , and E_{xp2} are diagonal matrices, with:

$$\begin{cases} P_{2(i,i)}^+ = \frac{1 + \text{sign}(P_{2(i)})}{2}, & P_{2(i,i)}^- = \frac{1 - \text{sign}(P_{2(i)})}{2} \\ E_{xp2(i,i)} = e^{-|\dot{q}_{2(i)}|/\dot{q}_s} \end{cases} \quad (34)$$

The identification gives the values of the load-dependent friction parameters for the joint 2 (Table 1).

The same method is applied to the joints 1 and 3 and one gets all friction parameters which are given in the Table 2.

TABLE 1
IDENTIFIED FRICTION PARAMETERS FOR JOINT 2

Parameters	Identified Values	Standard deviation * 2	Relative deviation
$1 + \alpha_{m2}$	1.0084	0.0039	0.1952
a_{m2}	0.1928	0.0064	1.6699
$1 - \alpha_{g2}$	0.8824	0.0040	0.2269
a_{g2}	0.2581	0.0065	1.2640

TABLE 2
IDENTIFIED FRICTION PARAMETERS FOR THE JOINTS 1 TO 3

Parameters \ j	1	2	3
$\dot{q}_s j$	0.1	0.1	0.15
$1 + \alpha_{mj}$	1.0717	1.0084	1.4241
a_{mj}	0.1524	0.1928	0.3170
$1 - \alpha_{gj}$	0.8460	0.8824	0.5377
a_{gj}	0.0909	0.2581	0.5039

E. Third Identification Step

A global identification of the 3 joints is carried out, with concatenation of all measurements: measurements joint by joint and measurements with all joints moving together. To concatenate the samples with different additional payloads fixed on the robot extremity, one defines for each joint j , the term $\tau_{maj(k)}$ which is the output torque due to the additional mass k , applied on joint j . This torque is calculated thanks to known inertial and gravity parameters obtained by masses

and dimensions measurements and CAD. Thus, each τ_{maj} depends on the additional mass and on the positions, velocities and accelerations of all joints.

One identifies first the usual model. The minimal inverse dynamic model is the same as in (7), except that one adds a column in the minimal regressor D , and 4 parameters in χ :

$$D_{usual} = \begin{bmatrix} \tau_{ma1} & 0 & 0 \\ D & 0 & \tau_{ma2} & 0 \\ 0 & 0 & 0 & \tau_{ma3} \end{bmatrix} \quad (35)$$

$$\chi_{usual} = [\chi^T \quad One_1 \quad One_2 \quad One_3]^T \quad (36)$$

with $One_j = \frac{\tau_{maje}}{\tau_{maj}}$, where τ_{maje} is the estimation of the torque τ_{maj} by the identification. If the model is well identified, each parameter One_j should be found close to one.

Then, one identifies the proposed model. The minimal inverse dynamic model is written from the usual one. At a first stage, one modifies the minimal regressor with the friction coefficients identified in step 2:

$$D_{new(j,k)} = (P_j^+ (I + \alpha_{mj} + a_{mj} E_{spj}) + P_j^- (I - \alpha_{gj} - a_{gj} E_{spj})) D_{usual(j,k)} \quad (37)$$

if χ_k is an inertial or a gravity parameter (that is to say one of the $XX, XY, XZ, YY, YZ, ZZ, MX, MY, MZ, m, Ia$, or One),

$$D_{new(j,k)} = D_{usual(j,k)} \text{ otherwise.}$$

At a second stage, one deals with the other friction parameters: the parameters F_{Cj} and their corresponding columns in D_{new} are first removed. Then instead, one adds the parameters β_{mj} , b_{mj} , β_{gj} , and b_{gj} and their corresponding columns in D_{new} :

- if β_{mj} is the k^{th} parameter in χ_{new} , then the column k of D_{new} is defined as follows:

$$D_{new(j,k)} = \begin{cases} 0 & \text{if } k \neq j \\ P_j^+ \text{sign}(\dot{q}_j) & \text{if } k = j \end{cases} \quad (38)$$

- if b_{mj} is the k^{th} parameter in χ_{new} , then the column k of D_{new} is defined as follows:

$$D_{new(j,k)} = \begin{cases} 0 & \text{if } k \neq j \\ P_j^+ E_{spj} \text{sign}(\dot{q}_j) & \text{if } k = j \end{cases} \quad (39)$$

- if β_{gj} is the k^{th} parameter in χ_{new} , then the column k of D_{new} is defined as follows:

$$D_{new(j,k)} = \begin{cases} 0 & \text{if } k \neq j \\ P_j^- \text{sign}(\dot{q}_j) & \text{if } k = j \end{cases} \quad (40)$$

- if b_{gj} is the k^{th} parameter in χ_{new} , then the column k of

D_{new} is defined as follows:

$$D_{new(j,k)} = \begin{cases} 0 & \text{if } k \neq j \\ P_j^- E_{spj} \text{sign}(\dot{q}_j) & \text{if } k = j \end{cases} \quad (41)$$

For this model too, the parameters One_j should be found close to one. Both models are compared using the same measurements and the LS technique.

F. Results

The significant values identified with usual IDM and OLS regressions are given in Table 3 and those with the new IDM in Table 4 (the parameters with a large relative deviation are not significant and have been eliminated). Moreover, Table 5 presents the relative norm of errors $\|\rho\|/\|Y\|$ and the standard deviation for the two models.

TABLE 3
IDENTIFIED VALUES WITH USUAL FRICTION MODEL

Parameters	Identified Values	Standard deviation * 2	Relative deviation
ZZ_{1R}	1.3788	0.0049	0.3526
XX_{2R}	-0.5813	0.0125	2.1428
ZZ_{2R}	1.1214	0.0037	0.3279
MX_{2R}	2.1369	0.0025	0.1184
ZZ_{3R}	0.2322	0.0019	0.7977
MY_{3R}	-0.6429	0.0023	0.3521
F_{S1}	4.4425	0.0037	0.0837
F_{V1}	7.8791	0.0147	0.1867
F_{S2}	6.5695	0.0068	0.1042
F_{V2}	4.4636	0.0156	0.3501
F_{S3}	6.7221	0.0130	0.1930
F_{V3}	1.6279	0.0129	0.7950
One_1	1.3004	0.0154	1.1876
One_2	1.0004	0.0020	0.2001
One_3	1.1167	0.0059	0.5313

TABLE 4
IDENTIFIED VALUES WITH NEW FRICTION MODEL

Parameters	Identified Values	Standard deviation * 2	Relative deviation
ZZ_{1R}	1.3041	0.0046	0.3549
XX_{2R}	-0.5749	0.0119	2.0742
ZZ_{2R}	1.2399	0.0032	0.2572
MX_{2R}	2.2137	0.0023	0.1028
ZZ_{3R}	0.2448	0.0013	0.5302
MY_{3R}	-0.5594	0.0016	0.2878
β_{m1}	5.3913	0.0076	0.1417
b_{m1}	-2.1524	0.0166	0.7719
F_{V1}	6.7915	0.0155	0.2279
β_{m2}	6.1698	0.0157	0.2543
b_{m2}	3.5588	0.0169	0.4749
β_{g2}	-2.8371	0.0361	1.2726
b_{g2}	7.4121	0.0393	0.5303
F_{V2}	4.4877	0.0142	0.3159
β_{m3}	5.5496	0.0203	0.3660
b_{m3}	4.2601	0.0120	0.2825
β_{g3}	-3.0153	0.0440	1.4608
F_{V3}	1.4561	0.0103	0.7045
One_1	1.3768	0.0143	1.0406
One_2	0.9962	0.0015	0.1551
One_3	1.0145	0.0029	0.2865

TABLE 5
MODELS COMPARISON

	Relative norm of error	Standard deviation
Usual Model	0.08913	1.3853
New Model	0.07042	1.3064

For each model and each joint, one plots a direct validation comparing the actual τ with its predicted value $W\hat{\lambda}$. The graphs Fig. 6 and Fig. 7 show the input torque for movements done with the payload of 2.2173 kg and with trajectories described by the graphs of the velocities Fig. 5: velocities between 40% and 80% of the nominal velocity for joint 1, velocity at 0.5% of the nominal velocity for joint 2, and velocities between 2% and 6% of the nominal velocity for joint 3. The graphs Fig. 6 are obtained for the usual model and the graphs Fig. 7 for the new model: the measured input torque is plotted in black, the estimated torque is plotted in light-gray and the error is plotted in dark-gray.

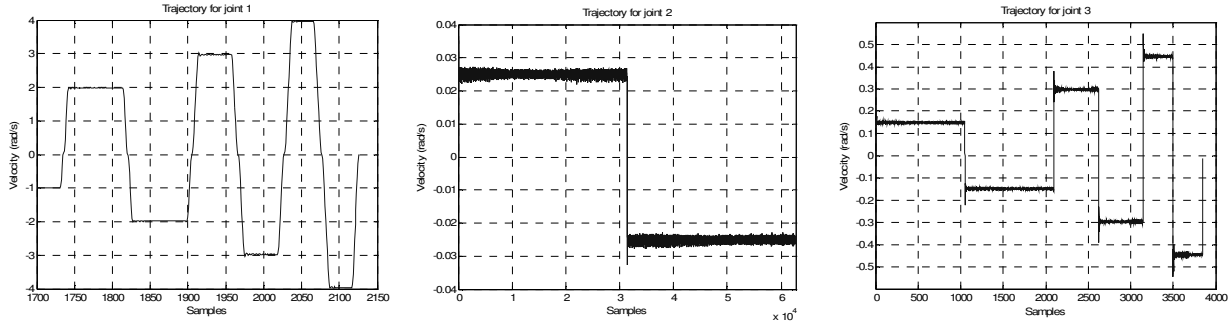


Fig. 5. Velocities of joints 1, 2 and 3 for the trajectories used in the torque comparison.

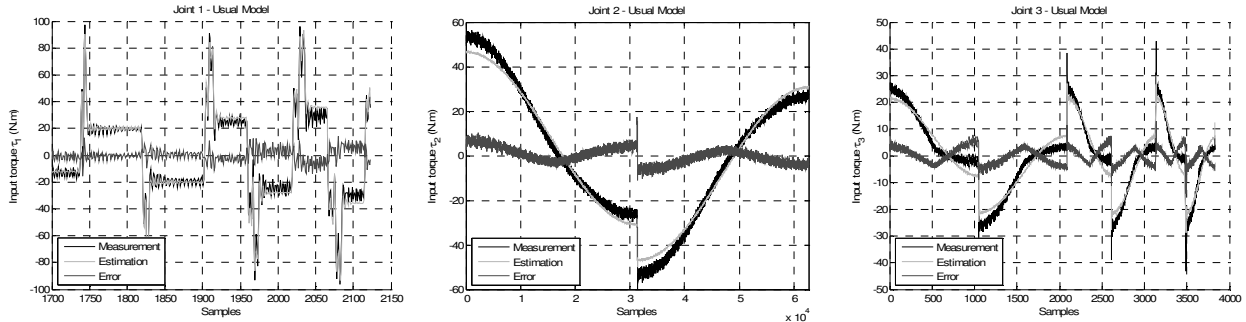


Fig. 6. Comparison between measurement and estimation for the usual model - Joints 1, 2 and 3.

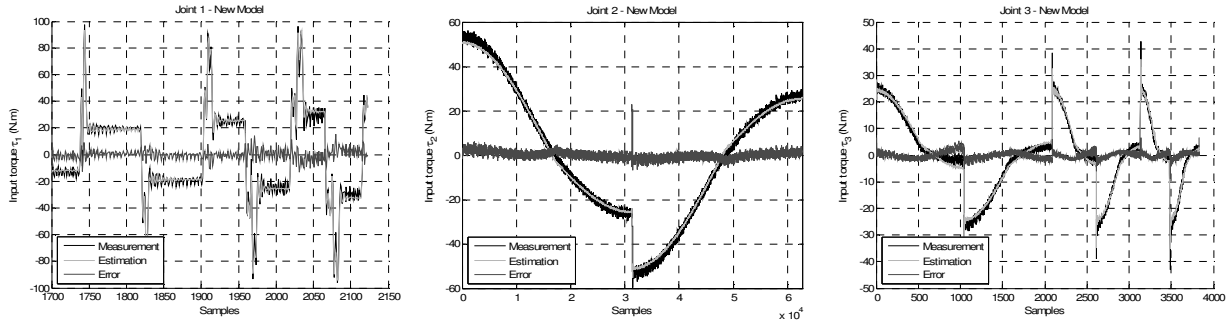


Fig. 7. Comparison between measurement and estimation for the new model - Joints 1, 2 and 3.

V. DISCUSSION

The parameters of both models are identifiable (low standard deviation). The parameters One_j are close to one which means that the additional payloads are well-identified by the models. As one can see in Table 5, the relative norm of error for the global identification is low. One observes a decrease of 20% in the relative norm of errors between the usual model and the new one. This difference is not very large because all measurements were used for the global identification: low and high velocities and low and high masses for the payload. The improvement is mostly important for low velocities and high load variation, whereas the models are equivalent at high velocity and low load variation.

The joint 1 has no load variation due to gravity, as it is vertical. Thus, the new model will be useful for the joint 1 at very low velocities (Stribeck effect) or when there are inertial variations: Fig. 6 and Fig. 7 show the input torque for a movement with high accelerations and velocities.

One sees an improvement especially for the highest velocity.

For the joint 2, Fig. 6 and Fig. 7 presents a comparison between the models, and for a movement at very low velocity, to show the improvement due to the modeling of the Stribeck effect. When the velocity increases, the improvement decreases but there is still an improvement with the new model due to the load-dependence. This one is not so important for the joint 2, as for the joint 3, as one can see in the Table 2: the parameters α_{m_2} and α_{g_2} are closer to 0 than the parameters α_{m_3} and α_{g_3} .

For the joint 3, one observes (Fig. 6 and Fig. 7) an important improvement thanks to the modeling of the load-dependence of friction. This modeling is very important at low velocity as the dry friction is predominant.

The identification of the new model is carried out with three steps, is more time-consuming and the setting up must be adapted for the measurements with additional masses. However, this model is valid for all type of movement: low and high velocities, low and high loads. For some movements, it is equivalent to the usual model, whereas for others (low velocities or high load variation), it brings a real improvement.

The proposed model is important for example in teleoperation, where the robots work at reduced velocity and can carry payloads or perform tasks with the effector subjected to external forces.

VI. CONCLUSION

This paper has presented a new dry friction model, with load- and velocity-dependence, and its identification method for a multi-dof robot. The inverse dynamic model and the identification of its parameters have been successfully validated on the 3 first joints of an industrial robot. As a result, one observes an improvement comparing to the usual model, for movements with large load variations and for movements at low velocity. Robots carrying important masses or with large inertial or gravity variations are concerned. The field of applications for which the new model can be very interesting is the telerobotics.

Future works concern the application of this model to slave robots for teleoperation and the use for torques monitoring and collision detection.

REFERENCES

- [1] C. G. Atkeson, C. H. An, and J. M. Hollerbach, "Estimation of Inertial Parameters of Manipulator Loads and Links", in *Int. J. of Robotics Research*, vol. 5(3), 1986, pp. 101-119.
- [2] J. Swevers, C. Ganseman, D. B. Tüchel, J. D. de Schutter, and H. Van Brussel, "Optimal Robot excitation and Identification", *IEEE Trans. on Robotics and Automation*, vol. 13(5), 1997, pp. 730-740.
- [3] P. K. Khosla and T. Kanade, "Parameter Identification of Robot Dynamics", in *Proc. 24th IEEE Conf. on Decision Control*, Fort-Lauderdale, December 1985.
- [4] M. Prüfer, C. Schmidt, and F. Wahl, "Identification of Robot Dynamics with Differential and Integral Models: A Comparison", in *Proc. 1994 IEEE Int. Conf. on Robotics and Automation*, San Diego, California, USA, May 1994, pp. 340-345.
- [5] B. Raucent, G. Bastin, G. Campion, J. C. Samin, and P. Y. Willems, "Identification of Barycentric Parameters of Robotic Manipulators from External Measurements", *Automatica*, vol. 28(5), 1992, pp. 1011-1016.
- [6] M. Gautier, "Identification of robot dynamics", in *Proc. IFAC Symp. On Theory of Robots*, Vienna, Austria, December 1986, pp. 351-356.
- [7] M. Gautier, "Dynamic identification of robots with power model", in *Proc. IEEE Int. Conf. on Robotics and Automation*, Albuquerque, 1997, pp. 1922-1927.
- [8] M. Gautier and P. H. Poinet, "Extended Kalman filtering and weighted least squares dynamic identification of robot", *Control Engineering Practice*, 2001.
- [9] W. Khalil, M. Gautier, and P. Lemoine, "Identification of the payload inertial parameters of industrial manipulators", *IEEE Int. Conf. on Robotics and Automation*, Roma, Italia, April 2007, pp. 4943-4948.
- [10] H. Kawasaki and K. Nishimura, "Terminal-link parameter estimation and trajectory control of robotic manipulators", *IEEE J. of Robotics and Automation*, vol. RA-4(5), pp. 485-490, 1988.
- [11] W. Khalil and E. Dombre, *Modeling, identification and control of robots*. Hermes Penton, London, 2002.
- [12] M. Gautier and W. Khalil, "Direct calculation of minimum set of inertial parameters of serial robots", *IEEE Trans. on Robotics and Automation*, vol. RA-6(3), 1990, pp. 368-373.
- [13] M. Gautier, "Numerical calculation of the base inertial parameters", *J. of Robotic Systems*, vol. 8(4), August 1991, pp. 485-506.
- [14] P. P. Restrepo and M. Gautier, "Calibration of drive chain of robot joints", in *Proc. 4th IEEE Conf. on Control Applications*, Albany, 1995, pp. 526-531.
- [15] A. Gogoussis and M. Donath, "Coulomb friction effects on the dynamics of bearings and transmissions in precision robot mechanisms", in *Proc. IEEE Int. Conf. on Robotics and Automation*, Philadelphia, Pennsylvania, April 1988, vol. 3, pp. 1440-1446.
- [16] M. E. Dohring, E. Lee, and W. S. Newman, "A load-dependent transmission friction model: theory and experiments", in *Proc. IEEE Int. Conf. on Robotics and Automation*, Atlanta, Georgia, May 1993, vol. 3, pp. 430-436.
- [17] C. Pelchen, C. Schweiger, and M. Otter, "Modeling and simulation the efficiency of gearboxes and of planetary gearboxes", in *Proc. 2nd International Modelica Conference*, Oberpfaffenhofen, Germany, March 2002, pp. 257-266.
- [18] N. Chaillet, G. Abba, and E. Ostertag, "Double dynamic modelling and computed-torque control of a biped robot", in *Proc. IEEE/RSJ/CI Int. Conf. on Intelligent Robots and Systems, 'Advanced Robotics Systems and the Real World'*, Munich, Germany, September 1994, vol. 2, pp. 1149-1155.
- [19] P. Garrec, J.-P. Fricconneau, Y. Measson, and Y. Petrot, "ABLE, an Innovative Transparent Exoskeleton for the Upper-Limb", *IEEE Int. Conf. on Intelligent Robots and Systems*, Nice, France, September 2008, pp. 1483-1488.
- [20] H. Olsson, K. J. Aström, C. Canudas de Wit, M. Gäfvert and P. Lischinsky, "Friction Models and Friction Compensation", in *European Journal of Control*, vol 4(3), 1998, pp. 176-195.
- [21] B. Armstrong-Hélouvy, *Control of machines with friction*. Springer, Boston, 1991.
- [22] J. Swevers, F. Al-Bender, C. G. Ganseman, and T. Prajogo, "An Integrated Friction Model Structure with Improved Presliding Behavior for Accurate Friction Compensation", *IEEE Trans. on Automatic Control*, vol. 45(4), 2000, pp. 675-686.
- [23] P. Hamon, M. Gautier, and P. Garrec, "Dynamic Identification of Robot with a Dry Friction Model Depending on Load and Velocity", *IEEE Int. Conf. on Intelligent Robots and Systems*, Taipei, Taiwan, October 2010.
- [24] P. Hamon, M. Gautier, P. Garrec, and A. Janot, "Dynamic Modeling and Identification of Joint Drive with Load-Dependent Friction Model", *IEEE Int. Conf. on Advanced Intelligent Mechatronics*, Montreal, Canada, July 2010.
- [25] Mathworks website, <http://www.mathworks.com/>
- [26] Stäubli website, <http://www.staubli.com/>